Coral Sr-U Thermometry

Thomas M. DeCarlo[1]*, Glenn A. Gaetani[2], Anne L. Cohen[2], Gavin L. Foster[3], Alice E. Alpert[1], and Joseph Stewart[3]

[1] Massachusetts Institute of Technology / Woods Hole Oceanographic Institution Joint Program in Oceanography / Applied Ocean Science and Engineering, Woods Hole Oceanographic Institution, Woods Hole, MA 02543, U.S.A.

[2] Woods Hole Oceanographic Institution, Woods Hole, MA 02543, U.S.A.

[3] Ocean and Earth Science, University of Southampton, Southampton SO14 3ZH, UK.

* Corresponding author: tdecarlo@whoi.edu

Key Points

1) Coral biomineralization confounds geochemical temperature proxies based on single element/Ca ratios

2) U/Ca ratios track the calcifying fluid variations that distort the temperature dependence of Sr/Ca

3) Coral Sr/Ca and U/Ca ratios used in tandem improves accuracy of seawater temperature reconstructions

Abstract

Coral skeletons archive past climate variability with unrivaled temporal resolution. However, extraction of accurate temperature information from coral skeletons has been limited by "vital effects", which confound, and sometimes override, the temperature dependence of geochemical proxies. We present a new approach to coral paleothermometry based on results of abiogenic precipitation experiments interpreted within a framework provided by a quantitative model of the coral biomineralization process. *DeCarlo et al.,* [2015a] investigated temperature and carbonate chemistry controls on abiogenic partitioning of Sr/Ca and U/Ca between aragonite and seawater and modeled the sensitivity of skeletal composition to processes occurring at the site of calcification. The model predicts that temperature can be accurately reconstructed from coral skeleton by combining Sr/Ca and U/Ca ratios into a new proxy, which we refer to hereafter as the Sr-U thermometer. Here, we test the model predictions with measured Sr/Ca and U/Ca ratios of fourteen *Porites* sp. corals collected from the tropical Pacific Ocean and the Red Sea, with a subset also analyzed using the boron isotope ($\delta^{11}B$) pH

35 proxy. Observed relationships among Sr/Ca, U/Ca, and $\delta^{11}B$, agree with model
36 predictions, indicating that the model accounts for the key features of the coral
37 biomineralization process. By calibrating to instrumental temperature records, we show
38 that Sr-U captures 93% of mean annual temperature variability (26-30 °C) and has a
39 standard deviation of prediction of 0.5 °C, compared to 1 °C using Sr/Ca alone. The Sr-U
40 thermometer may offer significantly improved reliability for reconstructing past ocean
41 temperatures from coral skeletons.
42

43 **1. Introduction**

44 Since 1900, global mean surface temperatures have increased at an average rate of
45 ~0.08 °C per decade, and state-of-the-art general circulation models (GCMs) project
46 further warming of 1-4 °C by the end of this century in response to anthropogenic
47 greenhouse gas (GHG) emissions [*Meehl et al.*, 2012; *Stocker et al.*, 2013]. These
48 projections depend in large part on estimates of "climate sensitivity", the sensitivity of
49 Earth's temperature to a doubling of atmospheric CO_2, and there is substantial
50 uncertainty in these estimates. Natural oscillations in atmospheric and oceanic circulation
51 occurring on inter-annual (*e.g.* El Niño Southern Oscillation), multi-decadal (*e.g.* Pacific
52 Decadal Oscillation), and centennial (*e.g.* the Little Ice Age) timescales can partially
53 obscure climate sensitivity, and how these modes of variability interact with, and possibly
54 change, under GHG forcing remain uncertain [*Wittenberg*, 2009; *Stevenson et al.*, 2012;
55 *Emile-Geay et al.*, 2013; *Li et al.*, 2013; *Meehl et al.*, 2014]. Multi-century long records
56 of temperature can help to resolve these issues by enabling characterization of internal

57 variability and isolation of secular temperature trends driven by external forcing (*e.g.*,
58 GHGs).

59 Direct observations of temperature, however, extend back only as far as the mid-
60 19th century [*Smith et al.*, 2008]. Furthermore, in regions such as the central tropical
61 Pacific Ocean, where sparse observations exist prior to 1950 [*Giese and Ray*, 2011],
62 estimates of 20th century warming vary up to a factor of two [*Nurhati et al.*, 2011;
63 *Solomon and Newman*, 2012; *Emile-Geay et al.*, 2013]. These limits to the length and
64 reliability of instrumental records make it difficult to constrain the range of natural
65 variability, the degree of 20th century warming, and the climate sensitivity to GHG
66 forcing. Accurate proxy temperature reconstructions offer the only way to extend the
67 relatively short observational period further into the past and overcome the limitations of
68 instrumental temperature records.

69 The skeletons of long-lived reef-building corals are a promising archive of this
70 information. Distributed across the tropics at shallow water depths, corals are exposed to
71 the sea surface temperature (SST), and accrete their skeletons in alternating high- and
72 low-density bands that provide intrinsic, high-resolution time markers extending
73 hundreds of years into the past [*Buddemeier et al.*, 1974]. As corals grow, the
74 geochemistry of their skeletal aragonite is sensitive to fluctuations in environmental
75 conditions, including temperature. The most common coral-based temperature proxy
76 currently in use is the Sr/Ca thermometer, which exploits the inverse relationship
77 between Sr/Ca and water temperature [*Kinsman and Holland*, 1969; *Smith et al.*, 1979;
78 *Gaetani and Cohen*, 2006; *DeCarlo et al.*, 2015a]. Typically, Sr/Ca ratios are first
79 calibrated with modern instrumental SST records to establish a coral-specific Sr/Ca-

temperature relationship, and then applied down-core to the older skeleton of the same coral, or in some cases to fossil corals, in order to reconstruct past SST [*Smith et al.*, 1979; *Felis et al.*, 2009; *Hereid et al.*, 2013; *Tierney et al.*, 2015; *Toth et al.*, 2015].

However, problems arise because SST is not the only factor that influences coral Sr/Ca. The biomineralization process affects Sr/Ca ratios and can do so independently of any changes in temperature. These biological influences are known as "vital effects", and are obvious in the comparison between coral and abiogenic aragonites. The temperature dependence of Sr/Ca in coral skeleton (-0.05 to -0.08 mmol mol^{-1} Sr/Ca per °C) is significantly stronger than that of abiogenic aragonite (-0.039 to -0.044 mmol mol^{-1} Sr/Ca per °C) [*Cohen et al.*, 2002; *Gaetani and Cohen*, 2006; *Gaetani et al.*, 2011; *DeCarlo et al.*, 2015a], and Sr/Ca-temperature relationships derived for different corals can vary widely. For *Porites* corals, a given Sr/Ca ratio can correspond to a range of temperatures in excess of 10 °C depending on which calibration equation is applied [*Corrège*, 2006; *Gaetani et al.*, 2011]. The influences of vital effects on Sr/Ca ratios are also borne out in coral-based SST reconstructions, which repeatedly fail to capture observed temperature trends [*Grove et al.*, 2013; *Storz et al.*, 2013; *Karnauskas et al.*, 2015; *Alpert et al.*, 2016], and often decouple from observed SST by > 4 °C [*Marshall and McCulloch*, 2002; *Felis et al.*, 2009; *Wu et al.*, 2014].

Evidence suggests that these Sr/Ca vital effects arise because corals accrete their skeleton within an isolated calcifying space [*Cohen et al.*, 2006; *Gaetani and Cohen*, 2006]. As aragonite crystals nucleate from the fluid within this space, the elemental composition of the fluid changes. Element ratios that are elevated in aragonite relative to the fluid (*e.g.*, Sr/Ca) become progressively lower in the fluid as precipitation proceeds.

103 This is known as Rayleigh fractionation [*Cohen et al.*, 2006; *Gaetani and Cohen*, 2006].
104 At a given temperature, the Sr/Ca ratio of the aragonite will monotonically decrease as
105 precipitation proceeds, in response to changes in the Sr/Ca ratio of the calcifying fluid.
106 Fluctuations in calcifying fluid carbonate ion concentration ($[CO_3^{2-}]$) likely drive
107 variations in the amount of aragonite precipitation and thus cause fluctuations in the
108 magnitude of the Rayleigh fractionation vital effect [*Cohen et al.*, 2009; *Gagnon et al.*,
109 2013]. Accurate coral-based temperature proxies must therefore account for this process
110 in order to isolate the temperature component of geochemical variability in the skeleton.
111 Abiogenic aragonite precipitation experiments showed that U/Ca ratios of
112 aragonite precipitated from seawater decrease as carbonate ion concentrations increase
113 [*DeCarlo et al.*, 2015a], and thus U/Ca ratios have potential to account for the vital
114 effects that influence Sr/Ca ratios. Here, we use coral Sr/Ca and U/Ca ratios interpreted
115 within the context of the biomineralization model developed by *DeCarlo et al.,* [2015a]
116 to test the hypothesis that Sr/Ca and U/Ca ratios can be used in tandem to accurately
117 reconstruct past seawater temperature. We use data from fourteen corals collected in the
118 tropical Pacific Ocean and the Red Sea, for which instrumental temperature data are
119 available for comparison. In a subset of these corals, we also measured boron isotopic
120 composition (a proxy for pH) to test our hypothesis that vital effects in coral Sr/Ca ratios
121 arise from processes occurring during biomineralization.
122
123 **2. Methods**
124 **2.1. Coral records**

125 Coral skeleton cores were collected from massive *Porites* sp. colonies using
126 underwater pneumatic drills. Two cores were collected from the central Red Sea near
127 Jeddah, Saudi Arabia, two from Palmyra Atoll, four from Jarvis Island, and six in the
128 Republic of Palau (Figure 1). The mean annual temperatures at which each coral lived
129 were acquired for time periods coincident with element ratio measurements using the
130 NOAA Optimum Interpolation (OI) SST dataset [*Reynolds et al.*, 2002]. Temperature
131 was compared between NOAA-OI and *in situ* temperature loggers deployed on each reef
132 at the water depths of coral samples, and a correction was applied to NOAA-OI to
133 account for any mean bias in temperature during overlapping time periods with the *in*
134 *situ* loggers (Figure 1).

135 Coral cores were scanned with a Siemens Volume Zoom Spiral Computerized
136 Tomography (CT) scanner to determine skeletal density. Annual density banding was
137 used to develop an age model for each coral (Figure 2). Slabs were cut from cores with a
138 water-cooled diamond wafering blade and cleaned for 15 minutes in an ultrasonic bath
139 filled with 18.2 MΩ deionized water before drying at 60 °C for at least 24 hours.
140 Subsamples of approximately 100 μg were drilled from slabs with a fine-tipped,
141 diamond-impregnated drillbit at 0.5 to 1.25 mm (approximately monthly) resolution.
142 Sampling followed primary growth axes, tracking the growth paths of corallites.

143 **2.2 Trace elements**

144 Coral powders were dissolved in 5% trace metal grade nitric acid and counts of
145 ^{48}Ca, ^{88}Sr, and ^{238}U were measured in low-resolution on a Thermo Element2 inductively
146 coupled plasma mass spectrometer (ICP-MS) at Woods Hole Oceanographic Institution.
147 External precision (one relative standard deviation) was 0.4% for Sr/Ca and 0.8% for

U/Ca, determined via repeated measurements of a secondary coral standard treated as a sample. Jarvis data are reported in *Alpert et al.*, [2016]. Element ratio measurements were standardized to the JCp-1 coral standard [*Okai et al.*, 2002], which has nominal Sr/Ca and U/Ca ratios of 8.838 ± 0.042 mmol mol^{-1} and 1.192 ± 0.045 μmol mol^{-1}, respectively [*Hathorne et al.*, 2013]. JCp-1 analyses bracketed every eight sample analyses. Sr/Ca ratios were also measured repeatedly in standard materials derived from fish otoliths [*Yoshinaga et al.*, 2000; *Sturgeon et al.*, 2005] and the NBS-19 limestone [*Fernandez et al.*, 2011] to ensure consistency of our Sr/Ca calibrations. As reported in [*Alpert et al.*, 2016], the batch of JCp-1 used in this study was compared to High Purity Standards single element standards gravimetrically mixed to simulate coral skeleton (40 ppm Ca with variable concentrations of Mg, Sr, Ba, and U). Three aliquots of JCp-1 powder were dissolved and each analyzed in duplicate with resulting mean ± 1 σ for Sr/Ca of 8.87 ± 0.03 mmol mol^{-1} and U/Ca of 1.23 ± 0.01 μmol mol^{-1}.

2.3. Boron isotopes

Two pairs of corals, each pair collected from a single reef in Palau, were analyzed for boron isotopic composition. $\delta^{11}B$ was measured in splits of the same samples used for Sr/Ca and U/Ca analyses following the methods of *Foster et al.* [2008] and *Foster et al.* [2013]. Briefly, $\delta^{11}B$ splits were oxidatively cleaned at 80 °C in 1% H_2O_2 (buffered with 0.1 M NH_4OH) in the clean lab of the University of Southampton. Oxidatively cleaned samples were then subjected to a weak acid leach and dissolved in a minimum volume of 0.5 M HNO_3, and boron was then separated from the dissolved sample using Amberlite IRA 743 anion exchange resin in 20 μl micro-columns. The boron isotopic composition was determined using a Thermo Scientific Neptune multi-

collector ICP-MS at the University of Southampton normalized against NIST SRM 951. The long term precision (following *Henehan et al.,* [2013]) was better than ± 0.21‰ at 95% confidence, and during the course of this study repeat analysis of JCp-1 gave $\delta^{11}B$ of 24.2 ± 0.2‰ at 95% confidence. Calcifying fluid pH was calculated from measured $\delta^{11}B_{coral}$ as $pH = pK_B - \log\left(-\frac{\delta^{11}B_{seawater} - \delta^{11}B_{coral}}{\delta^{11}B_{seawater} - \alpha_B \delta^{11}B_{coral} - 1000(\alpha_B - 1)}\right)$ following *Zeebe and Wolf-Gladrow* [2001] where α_B is equal to 1.0272 [*Klochko et al.,* 2006], pK_B is estimated from temperature and salinity based on *Dickson* [1990], and $\delta^{11}B_{seawater}$ is assumed to be 39.6‰ (following *Foster et al.* [2010]) and representative of the ECF. For each coral we calculated the mean pH over 2008-2009 in order to facilitate comparison among corals.

2.4. Statistics

The relationship between Sr/Ca and U/Ca in our coral samples was examined using linear regression, and with analysis of covariance (ANCOVA) in which Sr/Ca is the dependent variable, U/Ca is the covariate, and coral colony is an independent factor. ANCOVA tests the significance of Sr/Ca to U/Ca correlation in our corals, while allowing the relationship between Sr/Ca and U/Ca to vary among coral colonies. We evaluated our data with ANCOVA both including and excluding an interaction between coral colony and U/Ca (*i.e.*, different slopes of Sr/Ca vs U/Ca for different corals). Differences in mean values of element ratios or calcifying fluid pH between corals were evaluated with two-sample t-tests. Linear regression was used to test for correlations between coral geochemical data and temperature. Throughout this study, significance is defined as $p < 0.05$. Coral trace element and boron isotope data are reported in the supplementary information.

3. Results and Discussion

3.1. Modeling vital effects

Vital effects on coral skeletal geochemistry are linked with the biomineralization process. Corals nucleate and grow the aragonite crystals that form their skeleton within an isolated space located beneath the calicoblastic epithelial cells [*Barnes*, 1970; *Venn et al.*, 2011]. Evidence from culture experiments with calcein dyes and solutions doped with biologically inert elements suggests that seawater transport into this space supplies the elements for crystallization [*Gagnon et al.*, 2012; *Tambutté et al.*, 2012]. Corals modify the carbonate chemistry of the incoming seawater - likely via alkalinity pumping [*Al-Horani et al.*, 2003; *Cohen and McConnaughey*, 2003; *Venn et al.*, 2011] - to induce aragonite precipitation. The modified seawater from which the aragonite crystals precipitate is referred to as the extracellular calcifying fluid (ECF). If calcification proceeds in an isolated (or semi-isolated) space, as microscopy [*Venn et al.*, 2011] and geochemical [*Cohen et al.*, 2006; *Gaetani and Cohen,* 2006] evidence suggests, there are critical implications for interpreting compositional variations in coral skeleton. Changes in the extent of precipitation from an isolated calcifying fluid would lead to variability of element ratios in coral skeletons as a result of Rayleigh fractionation. For many corals, more than half of the Sr/Ca variance has been attributed to such vital effects [*Cohen et al.*, 2002; *Gaetani et al.*, 2011].

To shed light on the origin of vital effects, and to potentially quantify their effects on the composition of coral skeleton, we can look to co-variability among multiple element ratios. The basis for a multi-element approach to coral

paleothermometry comes from laboratory experiments that determined the abiogenic controls on elemental partitioning between aragonite and seawater [*Gaetani and Cohen*, 2006; *Gabitov et al.*, 2008], and modeling studies that placed abiogenic partitioning of multiple elements within a coral biomineralization framework [*Cohen et al.*, 2006; *Cohen and Gaetani*, 2010; *Gaetani et al.*, 2011; *Gagnon et al.*, 2012]. Subsequent coral culture and modeling studies identified the importance of carbonate chemistry changes occurring within the ECF on the elemental composition of the skeleton [*Cohen et al.*, 2009; *Gagnon et al.*, 2013; *Tanaka et al.*, 2015]. *DeCarlo et al.*, [2015a] recently conducted laboratory precipitation experiments that characterized the abiogenic carbonate chemistry and temperature controls on Sr/Ca and U/Ca partitioning between aragonite and seawater. Previous studies consistently report positive correlations between coral Sr/Ca and U/Ca ratios [*Cardinal et al.*, 2001; *Hendy et al.*, 2002; *Quinn and Sampson*, 2002; *Fallon et al.*, 2003; *Sinclair et al.*, 2006; *Felis et al.*, 2009, 2012; *Jones et al.*, 2015]. However, correlations between Sr/Ca and U/Ca are not found in experimentally precipitated abiogenic aragonite, in which Sr/Ca is controlled by temperature and is insensitive to $[CO_3^{2-}]$, whereas U/Ca is controlled by $[CO_3^{2-}]$ but is insensitive to temperature [*DeCarlo et al.*, 2015a]. The correlations between Sr/Ca and U/Ca in coral skeletons must, therefore, derive from processes occurring during biomineralization.

Quantitative, geochemical models of the coral biomineralization process provide a framework within which the environmental drivers of variability in skeletal composition (*e.g.*, Sr/Ca sensitivity to SST) can be distinguished from vital effects that arise during biomineralization (*e.g.*, influence of Rayleigh fractionation on Sr/Ca).

240 *DeCarlo et al.,* [2015a] developed a forward biomineralization model that successfully
241 predicts Sr/Ca and U/Ca ratios of coral skeleton. Seawater exchange, alkalinity pumping,
242 and aragonite precipitation modify the elemental composition of the ECF (Figure 3).
243 Together, these processes influence the Sr/Ca and U/Ca ratios of the skeleton via
244 Rayleigh fractionation and changes in the ECF [CO_3^{2-}]. This combination of factors
245 produces a positive correlation between coral skeleton Sr/Ca and U/Ca ratios at a single
246 temperature, such that a given coral Sr/Ca ratio does not correspond to a unique
247 temperature (Figure 3). However, the modeling results also suggest a new approach for
248 deriving temperature from coral skeletons. Since U/Ca is sensitive to Rayleigh
249 fractionation – through variations in [CO_3^{2-}] – but not to temperature, a single U/Ca ratio
250 can serve as a benchmark with which to investigate variability in other element ratios
251 independent of vital effects driven by Rayleigh fractionation. Comparing Sr/Ca ratios
252 that correspond to a single U/Ca ratio should, therefore, isolate the temperature
253 component of the Sr/Ca signal (Figure 3).

254 **3.2. Development of Sr-U thermometry**

255 The implication of the biomineralization model is that Sr/Ca and U/Ca ratios in
256 coral skeleton can be combined to accurately reconstruct past seawater temperature.
257 Here, we use our coral Sr/Ca, U/Ca, and $\delta^{11}B$ data to test predictions from the
258 biomineralization model (Figure 3). The first prediction of the model is that Sr/Ca and
259 U/Ca are positively correlated within the skeleton of each coral colony. We found that
260 Sr/Ca is significantly positively correlated with U/Ca (ANCOVA including interaction
261 between coral colony and U/Ca, $r^2 = 0.86$) across all of our corals (Figures 4 and 5).
262 According to the model, corals that experience the same temperature may have different

263 Sr/Ca ratios, but we expect that any differences in Sr/Ca among such corals will be
264 positively correlated with U/Ca and inversely correlated with pH_{ECF} (Figure 3). We
265 tested this prediction using corals from Palau that have significantly different Sr/Ca
266 ratios even though they experienced the same temperatures (Figure 4 and supplementary
267 Figure S1). Within each pair of corals collected from a single reef and sampled over the
268 same time period (*i.e.*, that experienced the same temperatures), the pH_{ECF} is
269 significantly higher, and the U/Ca ratio is significantly lower, in the coral with lower
270 Sr/Ca (Figure 4), consistent with the model prediction (Figure 3).
271 The key prediction of the model for paleothermometry is that Sr/Ca and U/Ca
272 ratios can be used in tandem to accurately reconstruct temperature. In particular, here we
273 test the prediction that the Sr/Ca ratio of each coral corresponding to a specific U/Ca
274 ratio correlates with temperature (Figure 3). To do this, we select the median U/Ca ratio
275 among all of our coral data (1.1 μmol mol^{-1}), and we use the correlations between Sr/Ca
276 and U/Ca to estimate the Sr/Ca ratio, for each coral, that corresponds to this median
277 U/Ca ratio. We first regress Sr/Ca with U/Ca, separately for each coral:

278 $$\widehat{Sr/Ca} = m_i\,(U/Ca) + b_i \qquad (1)$$

279 where $\widehat{Sr/Ca}$ is the estimated Sr/Ca ratio from a given U/Ca ratio, m_i is the slope and b_i
280 is the intercept of ordinary least squares regression performed using the data of a single
281 coral *i* with Sr/Ca as the dependent variable and U/Ca the independent variable. We then
282 define Sr-U for each coral as the estimated Sr/Ca ratio at the median U/Ca ratio:

283 $$Sr\text{-}U_i = m_i(1.1) + b_i \qquad (2)$$

284 where a single $Sr\text{-}U_i$ value is estimated for each coral, *i*. Sr-U from the fourteen corals is
285 significantly correlated with mean annual temperature ($r^2 = 0.93$, Figure 5 and Table 1),

286 in agreement with the prediction of the biomineralization model. Temperature is
287 predicted from Sr-U according to the following calibration equation (± 1 standard error
288 of coefficients):
289 Temperature (°C) = (-11 ± 1)(Sr-U - 9) + (28.1 ± 0.1) (3)
290 where 9 is subtracted from Sr-U to center the regression about zero. Whereas equations
291 (1) and (2) are defined independently for each colony (*i.e.* the regression between Sr/Ca
292 and U/Ca is based on a particular coral record), the temperature sensitivity of Sr-U in
293 equation (3) is calibrated with all fourteen corals in our dataset. The standard deviation of
294 prediction of mean temperature for Sr-U is ± 0.5 °C and the root mean square error
295 between observed and predicted temperature is 0.4 °C, approximately half of the
296 uncertainty based on Sr/Ca alone (Figure 5).
297 In our ANCOVA, the intercept of the relationship between Sr/Ca and U/Ca varies
298 greatly among coral colonies (explaining 58% of total Sr/Ca variance). While differences
299 in the slope of the Sr/Ca and U/Ca relationship (*i.e.*, interaction between coral colony and
300 U/Ca) are significant, the slopes vary only slightly (explaining ~1% of total Sr/Ca
301 variance). This means that most (84%) of Sr/Ca variance is explained by regression to
302 U/Ca with a single slope applied to all corals, but with different intercepts (*i.e.*, offsets in
303 Sr/Ca among corals). Including the interaction term is statistically robust, but it has
304 potentially important ramifications for applying Sr-U outside of our calibration. The
305 strength of the correlation between Sr/Ca and U/Ca influences the ordinary least squares
306 slope, and thus, Sr-U could be sensitive to any effect of sampling resolution on the r^2
307 between Sr/Ca and U/Ca. Further, if we include the interaction term, we must define Sr-U
308 as the Sr/Ca ratio predicted at a certain U/Ca ratio, one that is within the range of our

dataset. Extrapolation to higher or lower U/Ca ratios would lead to small differences in the Sr/Ca to U/Ca slope among corals having a disproportionally large effect on Sr-U. Alternatively, similar results are produced when Sr-U is defined without the interaction term (*i.e.*, the slope of Sr/Ca and U/Ca is the same for all corals), which is implemented by replacing equations (2) and (3) with equations (4) and (5), respectively:

$$\text{Sr-U}_{parallel} = \overline{\text{Sr/Ca}} - 1.1107\ \overline{\text{U/Ca}} \qquad (r^2 = 0.84) \qquad (4)$$

$$\text{Temperature (°C)} = (-10 \pm 1)(\text{Sr-U}_{parallel} - 7.7) + (28.8 \pm 0.1) \qquad (r^2 = 0.91) \qquad (5)$$

where overbars indicate means and Sr/Ca and U/Ca are in units of mmol mol^{-1} and μmol mol^{-1}, respectively.

The theoretical basis for Sr-U thermometry is derived from the general relationships predicted by the model (Figure 3), which are consistent with coral data (Figures 4 and 5). Yet, it is critical to recognize that Sr-U is empirically regressed against temperature in a core-top calibration, which has two important implications for its application to corals outside of our calibration dataset. First, seasonal temperature variability likely contributes, in part, to coral Sr/Ca signals, so that the regression line fit between Sr/Ca and U/Ca for a particular coral (equation 1) captures this seasonal temperature variability in Sr/Ca in addition to variability imposed by vital effects. For this reason, Sr-U as defined here is correlated with mean annual temperature, and cannot yet be applied to reconstruct seasonal temperature variability. Second, we have defined Sr-U over the temperature range 26 °C to 30 °C based on approximately monthly sampling of *Porites* skeletons for Sr/Ca and U/Ca ratios calibrated with the JCp-1 coral standard. Existing Sr/Ca and U/Ca datasets from *Diploria* and *Porites* corals collected in the Atlantic and Pacific basins show correlations and slopes between these two ratios that are

similar to those found in our fourteen corals (Table 1), suggesting that the link between Sr/Ca and U/Ca is a consistent feature of coral skeletons. However, only corals analyzed in this study are used to calibrate Sr-U to temperature because previous paired measurements of modern coral Sr/Ca and U/Ca ratios are not traceable to JCp-1. We hypothesize that Sr-U is robust to a range of conditions, but we note that its accuracy for different coral genera, timescales, and mean annual temperatures outside of our calibration dataset should be validated with modern corals before application to paleo-reconstructions.

Sr-U thermometry uses U/Ca ratios to account for the vital effects on Sr/Ca that are driven by the carbonate chemistry, specifically the $[CO_3^{2-}]$, of the ECF. While ECF $[CO_3^{2-}]$ may be sensitive to seawater $[CO_3^{2-}]$, our model and our coral data indicate that variability in seawater chemistry does not impact the fidelity of the Sr-U thermometer. The modeled relationship between pH_{ECF} and U/Ca is sensitive to ambient seawater chemistry (Figure 3c), but the relationships among Sr/Ca, U/Ca, and temperature – for the most part – are not (Figure 3b). Since the start of the industrial era, anthropogenic emissions have increased atmospheric CO_2 from ~280 to ~400 ppmv, which has decreased seawater $[CO_3^{2-}]$ by ~40 μmol kg^{-1} [*Feely et al.*, 2009]. Our model predicts that this $[CO_3^{2-}]$ change alone has a negligible effect, less than 0.03 °C, on the accuracy of Sr-U thermometry (Figure 3), because it is mostly overridden by changes within the coral ECF. In fact, the corals used in this study were collected from reefs spanning a range of seawater carbonate chemistry [*DeCarlo et al.*, 2015b], including a two-fold difference in $[CO_3^{2-}]$ from 141 μmol kg^{-1} in the bays of Palau to 290 μmol kg^{-1} in the Red Sea [*Shamberger et al.*, 2014; *Bernstein et al.,* 2016]. Despite this wide range, residuals of the

355 Sr-U temperature calibration are not significantly correlated with seawater [CO_3^{2-}] (r^2 =
356 0.01), further highlighting that Sr-U is largely robust to changes in ambient seawater
357 carbonate chemistry.

358 **3.3. Implications for coral paleothermometry**

359 Coral paleothermometry began with the discoveries that seasonal cycles of $\delta^{18}O$
360 and Sr/Ca correlate with seawater temperature [*Weber and Woodhead*, 1972; *Smith et al.*,
361 1979]. The application of $\delta^{18}O$ as a direct temperature proxy is limited by its sensitivity to
362 salinity, leaving Sr/Ca as the preferred temperature proxy. However, once temperature
363 calibrations were developed for many different corals collected across the tropics, it
364 became clear that a single relationship between temperature and Sr/Ca does not exist
365 [*Corrège*, 2006]. A variety of approaches have been undertaken to resolve the non-
366 temperature controls on coral Sr/Ca ratios, including sampling along maximum growth
367 axes [*de Villiers et al.*, 1994], empirically regressing temperature to a variety of element
368 ratios [*Quinn and Sampson*, 2002], correcting with coral growth rate [*Saenger et al.*,
369 2008], accounting for "biosmoothing" [*Gagan et al.*, 2012], and replicating time series
370 [*DeLong et al.*, 2013]. However, no one approach has been able to resolve all of the Sr/Ca
371 vital effects, and Sr/Ca-based reconstructions continue to be plagued with unexplained
372 decouplings from temperature [*Wu et al.*, 2014].

373 Here, we present a new coral paleothermometer developed from a bottom-up
374 approach. Laboratory experiments were used to evaluate the temperature and carbonate
375 chemistry controls of aragonite Sr/Ca and U/Ca ratios, in the absence of any influence
376 from the coral polyp [*DeCarlo et al.*, 2015a]. The abiogenic partitioning results were then
377 placed within the framework of a biomineralization model to understand how corals

influence these element ratios while building their skeletons. Importantly, the model makes testable predictions of the relationships among coral skeleton Sr/Ca and U/Ca ratios, and pH_{ECF} (Figure 3), even though there are no correlations among these variables in experimentally precipitated abiogenic aragonite [*DeCarlo et al.*, 2015a]. These predictions are borne out in the composition of coral skeletons collected from different reefs across the Pacific Ocean and the Red Sea (Figures 4 and 5). The agreement between the model predictions and the coral data show that by combining information from Sr/Ca and U/Ca ratios, we are capturing the essential aspects of the biomineralization process that influence the elemental composition of the skeleton.

Sr-U offers a new approach to coral paleothermometry that is based on our understanding of the biomineralization process. Coral Sr/Ca ratios are sensitive to temperature, but that influence is subordinate to vital effects, which produce a range of Sr/Ca-temperature relationships (Figure 3). With the Sr-U thermometer, we incorporate information from two element ratios that are sensitive to different aspects of the biomineralization process – Sr/Ca, which is sensitive to temperature but also influenced by "vital effects" and U/Ca which records vital effects but is insensitive to temperature. In this way, U/Ca ratios can be used to normalize Sr/Ca ratios to a single temperature. Sr-U thermometry combines the temperature sensitivity of Sr/Ca with the vital effect sensitivity of U/Ca to extract temperature information from coral skeleton with accuracy not obtained by any other geochemical approach (Figure 5).

The utility of a temperature proxy is judged on its ability to provide accurate temperature information prior to the beginning of instrumental records. Currently, reconstruction of SST several centuries or more into the past is performed using Sr/Ca

401 calibrations developed with modern corals and applied to fossil samples [*DeLong et al.*,
402 2010; *Hereid et al.*, 2013; *Toth et al.*, 2015]. This approach is subject to significant
403 uncertainty as a result of the wide variability in Sr/Ca-temperature relationships derived
404 from coral colonies living at the same temperatures (Figure 4). For this reason, Sr-U
405 thermometry may prove particularly valuable for predicting SST from fossil corals that
406 lack a modern calibration period. The ability of the Sr-U thermometer to accurately
407 predict absolute temperature from different corals with a single calibration equation,
408 applicable over a broad spatial scale, separates it from thermometers based on Sr/Ca
409 alone.

410 Proxy reconstructions of past climate variability assume that the relationship
411 between the proxy and the climate variable of interest is constant with respect to space
412 and time. Coral Sr/Ca paleothermometry violates this assumption due to the influence of
413 vital effects on Sr/Ca-temperature relationships within the skeleton of single colonies.
414 Decoupling (or "breakdown") of the relationship between Sr/Ca and SST has been
415 observed in several studies [*Marshall and McCulloch*, 2002; *Felis et al.*, 2009; *Wu et al.*,
416 2014]. Perhaps the most drastic Sr/Ca breakdown was observed by *Felis et al.* [2009], in
417 which Sr/Ca ratios of a coral from the northwest Pacific implied that 1995-2000 was the
418 coolest period of the 20th century, when in fact it was the warmest. Critically, this Sr/Ca
419 breakdown is accompanied by a positive correlation with U/Ca ratios [*Felis et al.*, 2009].
420 Our model explains this breakdown: corals may shift along the Sr/Ca and U/Ca
421 trajectory driven by "vital effects", even in the absence of temperature changes (Figure 3).
422 The positive correlation between Sr/Ca and U/Ca reported by *Felis et al.* [2009] suggests
423 that observed Sr/Ca breakdowns are actually temporal variations in the coral

biomineralization process. This likely explains why many existing Sr/Ca records diverge from instrumental SST [*Grove et al.*, 2013; *Storz et al.*, 2013; *Wu et al.*, 2014], and potentially influences Sr/Ca records extended prior to the instrumental record for which no independent, direct observations of SST are available for comparison. When Sr/Ca breakdowns are observed during recent decades, instrumental SST allows us to identify that the Sr/Ca thermometer failed [*Felis et al.*, 2009; *Grove et al.*, 2013; *Storz et al.*, 2013; *Wu et al.*, 2014]. It is important to recognize, however, that when Sr/Ca is extended into the paleo-record, a Sr/Ca breakdown cannot be distinguished from a true temperature change unless coupled with U/Ca ratios to calculate Sr-U.

4. Conclusion

Coral skeletons are promising archives for high-resolution reconstructions of climate changes in the ocean over the past several millennia. However, application of geochemical temperature proxies – such as Sr/Ca – has proven difficult due to the confounding influence of physiological vital effects. Here we present a new coral paleothermometer, Sr-U, which uses U/Ca ratios to account for the influence of vital effects on Sr/Ca-temperature relationships. This approach significantly improves the accuracy of reconstructed temperature from coral skeleton. We calibrated Sr-U to temperature using a new dataset of Sr/Ca and U/Ca ratios measured in fourteen corals collected in the Pacific Ocean and the Red Sea spanning a mean annual temperature range of 26 °C to 30 °C. Sr-U thermometry has a standard deviation of prediction of only 0.5 °C, which is twice the accuracy compared to using Sr/Ca alone. Coral skeleton Sr/Ca and U/Ca ratios are routinely measured by ICP-MS, making the Sr-U thermometer

447 readily available to perform temperature reconstructions. With the improved accuracy,
448 and applicability of a single calibration equation to individual corals collected from
449 different locations, Sr-U thermometry has great potential for extending our limited
450 instrumental temperature records in the ocean.
451
452 **Acknowledgements**
453 We are grateful to G.P. Lohmann, Kathryn Pietro, Neal Cantin, NOAA Coral
454 Reef Ecosystem Division (CRED) and the Pacific Reef Assessment and Monitoring
455 Program (RAMP) for assistance with collection of coral cores. We also thank Scot
456 Birdwhistell (WHOI) and Meagan Gonneea (USGS) for assistance with ICP-MS
457 analyses, and Julie Arruda at the WHOI Computerized Scanning and Imaging Facility for
458 CT scanning of coral cores. The authors thank one anonymous reviewer for thoughtful
459 suggestions and Heiko Pälike for editorial handling. This work was supported by NSF
460 grants OCE-1338320 to G.A.G. and A.L.C., OCE-1031971 and OCE-1220529 to A.L.C.,
461 and by NSF Graduate Research Fellowships awarded to T.M.D and A.E.A. Coral
462 geochemical data are presented in the supporting information files.
463
464 **References**
465 Al-Horani, F. A., S. M. Al-Moghrabi, and D. De Beer (2003), The mechanism of
466 calcification and its relation to photosynthesis and respiration in the scleractinian
467 coral *Galaxea fascicularis*, *Mar. Biol.*, *142*(3), 419–426, doi:10.1007/s00227-002-
468 0981-8.
469 Alpert, A. E., A. L. Cohen, D. Oppo, T.M. DeCarlo, J. Gove, and C. Young (2016),

Comparison of equatorial Pacific sea surface temperature variability and trends with Sr/Ca records from multiple corals, *Paleoceanography*, *31*(2), 252-265, doi: 10.1002/2015PA002897.

Barnes, D. J. (1970), Coral skeletons: an explanation of their growth and structure, *Science*, *170*(3964), 1305–1308, doi:10.1126/science.170.3964.1305.

Bernstein, W. N., K. A. Hughen, C. Langdon, D. C. McCorkle, and S. J. Lentz (2016), Environmental controls on daytime net community calcification on a Red Sea reef flat, *Coral Reefs*, 1-15, doi:10.1007/s00338-015-1396-6.

Buddemeier, R. W., J. E. Maragos, and D. W. Knutson (1974), Radiographic studies of reef coral exoskeletons: rates and patterns of coral growth, *J. Exp. Mar. Biol. Ecol.*, *14*(2), 179–199, doi:10.1016/0022-0981(74)90024-0.

Cardinal, D., B. Hamelin, E. Bard, and J. Pätzold (2001), Sr/Ca, U/Ca and $\delta^{18}O$ records in recent massive corals from Bermuda: relationships with sea surface temperature, *Chem. Geol.*, *176*(1), 213–233, doi:10.1016/S0009-2541(00)00396-X.

Cohen, A. L., and G. A. Gaetani (2010), Ion partitioning and the geochemistry of coral skeletons: solving the mystery of the vital effect, *EMU Notes Mineral.*, *11*, 377–397, doi:10.1180/EMU-notes.10.11.

Cohen, A. L., and T. A. McConnaughey (2003), Geochemical Perspectives on Coral Mineralization, *Rev. Miner. Geochem.*, *54*(1), 151–187, doi:10.2113/0540151.

Cohen, A. L., K. E. Owens, G. D. Layne, and N. Shimizu (2002), The Effect of Algal Symbionts on the Accuracy of Sr/Ca Paleotemperatures from Coral, *Science*, *296*(5566), 331–333, doi:10.1126/science.1069330.

Cohen, A. L., G. A. Gaetani, T. Lundälv, B. H. Corliss, and R. Y. George (2006),

493 Compositional variability in a cold-water scleractinian, *Lophelia pertusa*: new
494 insights into "vital effects," *Geochemistry Geophys. Geosystems*, *7*(12), Q12004,
495 doi:10.1029/2006GC001354.
496 Cohen, A. L., D. C. McCorkle, S. de Putron, G. A. Gaetani, and K. A. Rose (2009),
497 Morphological and compositional changes in the skeletons of new coral recruits
498 reared in acidified seawater: Insights into the biomineralization response to ocean
499 acidification, *Geochemistry Geophys. Geosystems*, *10*(1), Q07005,
500 doi:10.1029/2009GC002411.
501 Corrège, T. (2006), Sea surface temperature and salinity reconstruction from coral
502 geochemical tracers, *Palaeogeogr. Palaeoclimatol. Palaeoecol.*, *232*(2), 408–428,
503 doi:doi:10.1016/j.palaeo.2005.10.014.
504 DeCarlo, T. M., G. A. Gaetani, M. Holcomb, and A. L. Cohen (2015a), Experimental
505 determination of factors controlling U/Ca of aragonite precipitated from seawater:
506 implications for interpreting coral skeleton, *Geochim. Cosmochim. Acta*, *162*, 151–
507 165, doi:doi:10.1016/j.gca.2015.04.016.
508 DeCarlo, T. M., A. L. Cohen, H. C. Barkley, Q. Cobban, C. Young, K. E. Shamberger, R.
509 E. Brainard, and Y. Golbuu (2015b), Coral macrobioerosion is accelerated by ocean
510 acidification and nutrients, *Geology*, *43*(1), 7–10, doi:10.1130/G36147.1.
511 DeLong, K. L., T. M. Quinn, C. Shen, and K. Lin (2010), A snapshot of climate
512 variability at Tahiti at 9.5 ka using a fossil coral from IODP Expedition 310,
513 *Geochemistry Geophys. Geosystems*, *11*(6), Q06005, doi:10.1029/2009GC002758.
514 DeLong, K. L., T. M. Quinn, F. W. Taylor, C. Shen, and K. Lin (2013), Improving coral-
515 base paleoclimate reconstructions by replicating 350years of coral Sr/Ca variations,

516 *Palaeogeogr. Palaeoclimatol. Palaeoecol.*, *373*, 6–24,
517 doi:10.1016/j.palaeo.2012.08.019.
518 Dickson, A. G. (1990), Thermodynamics of the dissociation of boric acid in synthetic
519 seawater from 273.15 to 318.15 K, *Deep Sea Res. Part A.*, *37*(5), 755–766,
520 doi:10.1016/0198-0149(90)90004-F.
521 Emile-Geay, J., K. M. Cobb, M. E. Mann, and A. T. Wittenberg (2013), Estimating
522 central equatorial Pacific SST variability over the past millennium. Part II:
523 reconstructions and implications, *J. Clim.*, *26*(7), 2329–2352,
524 doi:http://dx.doi.org/10.1175/JCLI-D-11-00511.1.
525 Fallon, S. J., M. T. McCulloch, and C. Alibert (2003), Examining water temperature
526 proxies in *Porites* corals from the Great Barrier Reef: a cross-shelf comparison,
527 *Coral Reefs*, *22*(4), 389–404, doi:10.1007/s00338-003-0322-5.
528 Feely, R. A., S. C. Doney, and S. R. Cooley (2009), Ocean acidification: present
529 conditions and future changes in a high-CO_2 world, *Oceanography*, *22*(4), 37–47,
530 doi:10.5670/oceanog.2009.95.
531 Felis, T., A. Suzuki, H. Kuhnert, M. Dima, G. Lohmann, and H. Kawahata (2009),
532 Subtropical coral reveals abrupt early-twentieth-century freshening in the western
533 North Pacific Ocean, *Geology*, *37*(6), 527–530, doi:10.1130/G25581A.1.
534 Felis, T., U. Merkel, R. Asami, P. Deschamps, E. Hathorne, M. Kölling, E. Bard, G.
535 Cabioch, N. Durand, and M. Prange (2012), Pronounced interannual variability in
536 tropical South Pacific temperatures during Heinrich Stadial 1, *Nat. Commun.*, *3*,
537 965, doi:10.1038/ncomms1973.
538 Fernandez, D. P., A. C. Gagnon, and J. F. Adkins (2011), An Isotope Dilution ICP-MS

539 Method for the Determination of Mg/Ca and Sr/Ca Ratios in Calcium Carbonate,
540 *Geostand. Geoanalytical Res.*, *35*(1), 23–37, doi:10.1111/j.1751-
541 908X.2010.00031.x.
542 Foster, G. L. (2008), Seawater pH, pCO_2 and [CO_3^{2-}] variations in the Caribbean Sea
543 over the last 130 kyr: A boron isotope and B/Ca study of planktic foraminifera,
544 *Earth Planet. Sci. Lett.*, *271*(1), 254–266, doi:10.1016/j.epsl.2008.04.015.
545 Foster, G. L., P. A. E. Pogge von Strandmann, and J. W. B. Rae (2010), Boron and
546 magnesium isotopic composition of seawater, *Geochemistry, Geophys. Geosystems*,
547 *11*(8), Q08015, doi:10.1029/2010GC003201.
548 Foster, G. L., B. Hönisch, G. Paris, G. S. Dwyer, J. W. B. Rae, T. Elliott, J. Gaillardet, N.
549 G. Hemming, P. Louvat, and A. Vengosh (2013), Interlaboratory comparison of
550 boron isotope analyses of boric acid, seawater and marine $CaCO_3$ by MC-ICPMS
551 and NTIMS, *Chem. Geol.*, *358*, 1–14, doi:10.1016/j.chemgeo.2013.08.027.
552 Gabitov, R. I., G. A. Gaetani, E. B. Watson, A. L. Cohen, and H. L. Ehrlich (2008),
553 Experimental determination of growth rate effect on U^{6+} and Mg^{2+} partitioning
554 between aragonite and fluid at elevated U^{6+} concentration, *Geochim. Cosmochim.*
555 *Acta*, *72*(16), 4058–4068, doi:10.1016/j.gca.2008.05.047.
556 Gaetani, G. A., and A. L. Cohen (2006), Element partitioning during precipitation of
557 aragonite from seawater: A framework for understanding paleoproxies, *Geochim.*
558 *Cosmochim. Acta*, *70*(18), 4617–4634, doi:10.1016/j.gca.2006.07.008.
559 Gaetani, G. A., A. L. Cohen, Z. Wang, and J. Crusius (2011), Rayleigh-Based, Multi-
560 Element Coral Thermometry: a Biomineralization Approach to Developing Climate
561 Proxies, *Geochim. Cosmochim. Acta*, *75*, 1920–1932,

562 doi:10.1016/j.gca.2011.01.010.
563 Gagan, M. K., G. B. Dunbar, and A. Suzuki (2012), The effect of skeletal mass
564 accumulation in *Porites* on coral Sr/Ca and $\delta^{18}O$ paleothermometry,
565 *Paleoceanography*, *27*(1), PA1203, doi:10.1029/2011PA002215.
566 Gagnon, A. C., J. F. Adkins, and J. Erez (2012), Seawater transport during coral
567 biomineralization, *Earth Planet. Sci. Lett.*, *329*, 150–161.
568 Gagnon, A. C., J. F. Adkins, J. Erez, J. M. Eiler, and Y. Guan (2013), Sr/Ca sensitivity to
569 aragonite saturation state in cultured subsamples from a single colony of coral:
570 Mechanism of biomineralization during ocean acidification, *Geochim. Cosmochim.*
571 *Acta*, doi:10.1016/j.gca.2012.11.038.
572 Giese, B. S., and S. Ray (2011), El Niño variability in simple ocean data assimilation
573 (SODA), 1871–2008, *J. Geophys. Res. Ocean.*, *116*(C2), C02024,
574 doi:10.1029/2010JC006695.
575 Grove, C. A., S. Kasper, J. Zinke, M. Pfeiffer, D. Garbe-Schönberg, and G. A. Brummer
576 (2013), Confounding effects of coral growth and high SST variability on skeletal
577 Sr/Ca: implicatiaons for coral paleothermometry, *Geochemistry, Geophys.*
578 *Geosystems*, *14*(4), 1277–1293, doi:10.1002/ggge.20095.
579 Hathorne, E. C. et al. (2013), Interlaboratory study for coral Sr/Ca and other element/Ca
580 ratio measurements, *Geochemistry, Geophys. Geosystems*, *14*(9), 3730–3750,
581 doi:10.1002/ggge.20230.
582 Hendy, E. J., M. K. Gagan, C. A. Alibert, M. T. McCulloch, J. M. Lough, and P. J. Isdale
583 (2002), Abrupt decrease in tropical Pacific sea surface salinity at end of Little Ice
584 Age, *Science*, *295*(5559), 1511–1514, doi:10.1126/science.1067693.

585 Henehan, M. J. et al. (2013), Calibration of the boron isotope proxy in the planktonic
586 foraminifera *Globigerinoides ruber* for use in palaeo-CO_2 reconstruction, *Earth*
587 *Planet. Sci. Lett.*, *364*, 111–122, doi:10.1016/j.epsl.2012.12.029.
588 Hereid, K. A., T. M. Quinn, F. W. Taylor, C. C. Shen, R. L. Edwards, and H. Cheng
589 (2013), Coral record of reduced El Niño activity in the early 15th to middle 17th
590 centuries, *Geology*, *41*(1), 51–54, doi:10.1130/G33510.1.
591 Jones, J. P., J. P. Carricart-Ganivet, R. Iglesias Prieto, S. Enríquez, M. Ackerson, and R.
592 I. Gabitov (2015), Microstructural variation in oxygen isotopes and elemental
593 calcium ratios in the coral skeleton of *Orbicella annularis*, *Chem. Geol.*, *419*, 192–
594 199, doi:10.1016/j.chemgeo.2015.10.044.
595 Karnauskas, K. B., A. L. Cohen, and E. J. Drenkard (2015), Comment on ``Equatorial
596 Pacific coral geochemical records show recent weakening of the Walker circulation''
597 by J. Carilli et al., *Paleoceanography*, *30*(5), 570–574, doi:10.1002/2014PA002753.
598 Kinsman, D. J. J., and H. D. Holland (1969), The co-precipitation of cations with $CaCO_3$-
599 IV. The co-precipitation of Sr^{2+} with aragonite between 16° and 96°C, *Geochim.*
600 *Cosmochim. Acta*, *33*(1), 1–17, doi:10.1016/0016-7037(69)90089-1.
601 Klochko, K., A. J. Kaufman, W. Yao, R. H. Byrne, and J. A. Tossell (2006),
602 Experimental measurement of boron isotope fractionation in seawater, *Earth Planet.*
603 *Sci. Lett.*, *248*(1), 276–285, doi:10.1016/j.epsl.2006.05.034.
604 Li, J., C. Sun, and F. Jin (2013), NAO implicated as a predictor of Northern Hemisphere
605 mean temperature multidecadal variability, *Geophys. Res. Lett.*, *40*(20), 5497–5502,
606 doi:10.1002/2013GL057877.
607 Marshall, J. F., and M. T. McCulloch (2002), An assessment of the Sr/Ca ratio in shallow

608 water hermatypic corals as a proxy for sea surface temperature, *Geochim.*
609 *Cosmochim. Acta*, *66*(18), 3263–3280, doi:10.1016/S0016-7037(02)00926-2.
610 Meehl, G. A. et al. (2012), Climate System Response to External Forcings and Climate
611 Change Projections in CCSM4, *J. Clim.*, *25*(11), 3661–3683, doi:10.1175/JCLI-D-
612 11-00240.1.
613 Meehl, G. A., H. Teng, and J. M. Arblaster (2014), Climate model simulations of the
614 observed early-2000s hiatus of global warming, *Nat. Clim. Chang.*, *4*(10), 898–902,
615 doi:10.1038/nclimate2357.
616 Nurhati, I. S., K. M. Cobb, and E. Di Lorenzo (2011), Decadal-scale SST and salinity
617 variations in the central tropical Pacific: Signatures of natural and anthropogenic
618 climate change, *J. Clim.*, *24*(13), 3294–3308,
619 doi:http://dx.doi.org/10.1175/2011JCLI3852.1.
620 Okai, T., A. Suzuki, H. Kawahata, S. Terashima, and N. Imai (2002), Preparation of a
621 New Geological Survey of Japan Geochemical Reference Material: Coral JCp-1,
622 *Geostand. Newsl.*, *26*(1), 95–99, doi:10.1111/j.1751-908X.2002.tb00627.x.
623 Quinn, T. M., and D. E. Sampson (2002), A Multiproxy Approach to Reconstructing Sea
624 Surface Conditions Using Coral Skeleton Geochemistry, *Paleoceanography*, *17*(4),
625 1062, doi:10.1029/2000PA000528.
626 Reynolds, R. W., N. A. Rayner, T. M. Smith, D. C. Stokes, and W. Wang (2002), An
627 improved in situ and satellite SST analysis for climate, *J. Clim.*, *15*(13), 1609–1625,
628 doi:http://dx.doi.org/10.1175/1520-0442(2002)015<1609:AIISAS>2.0.CO;2.
629 Saenger, C., A. L. Cohen, D. W. Oppo, and D. Hubbard (2008), Interpreting sea surface
630 temperature from strontium/calcium ratios in Montastrea corals: Link with growth

631 rate and implications for proxy reconstructions, *Paleoceanography*, *23*(3), PA3102,
632 doi:10.1029/2007PA001572.
633 Shamberger, K. E. F., A. L. Cohen, Y. Golbuu, D. C. McCorkle, S. J. Lentz, and H. C.
634 Barkley (2014), Diverse Coral Communities in Naturally Acidified Waters of a
635 Western Pacific Reef, *Geophys. Res. Lett., 41*(2), 499-504,
636 doi:10.1002/2013GL058489
637 Sinclair, D. J., B. Williams, and M. Risk (2006), A biological origin for climate signals in
638 corals—Trace element "vital effects" are ubiquitous in Scleractinian coral skeletons,
639 *Geophys. Res. Lett.*, *33*(17), doi:10.1029/2006GL027183.
640 Smith, S. V, R. W. Buddemeier, R. C. Redalje, and J. E. Houck (1979), Strontium-
641 calcium thermometry in coral skeletons., *Science*, *204*(4391), 404–7,
642 doi:10.1126/science.204.4391.404.
643 Smith, T. M., R. W. Reynolds, T. C. Peterson, and J. Lawrimore (2008), Improvements to
644 NOAA's Historical Merged Land-Ocean Surface Temperature Analysis (1880-
645 2006), *J. Clim.*, *21*(10), 2283–2296, doi:http://dx.doi.org/10.1175/2007JCLI2100.1.
646 Solomon, A., and M. Newman (2012), Reconciling disparate twentieth-century Indo-
647 Pacific ocean temperature trends in the instrumental record, *Nat. Clim. Chang.*, *2*(9),
648 691–699, doi:10.1038/nclimate1591.
649 Stevenson, S., B. Fox-Kemper, M. Jochum, R. Neale, C. Deser, and G. Meehl (2012),
650 Will there be a significant change to El Niño in the twenty-first century?, *J. Clim.*,
651 *25*(6), 2129–2145, doi:http://dx.doi.org/10.1175/JCLI-D-11-00252.1.
652 Stocker, T. F., D. Qin, G.-K. Plattner, M. Tignor, S. K. Allen, J. Boschung, A. Nauels, Y.
653 Xia, V. Bex, and P. M. Midgley (2013), *Climate change 2013: The physical science*

654 *basis*.
655 Storz, D., E. Gischler, J. Fiebig, A. Eisenhauer, and D. Garbe-Schönberg (2013),
656 Evaluation of oxygen isotope and Sr/Ca ratios from a Maldivian scleractinian coral
657 for reconstruction of climate variability in the northwestern Indian Ocean, *Palaios*,
658 *28*(1), 42–55, doi:10.2110/palo.2012.p12-034r.
659 Sturgeon, R. E., S. N. Willie, L. Yang, R. Greenberg, R. O. Spatz, Z. Chen, C. Scriver, V.
660 Clancy, J. W. Lam, and S. Thorrold (2005), Certification of a fish otolith reference
661 material in support of quality assurance for trace element analysis, *J. Anal. At.*
662 *Spectrom.*, *20*(10), 1067–1071, doi:10.1039/B503655K.
663 Tambutté, E., S. Tambutté, N. Segonds, D. Zoccola, A. Venn, J. Erez, and D. Allemand
664 (2012), Calcein labelling and electrophysiology: insights on coral tissue
665 permeability and calcification, *Proc. R. Soc. B Biol. Sci.*, *279*(1726), 19–27,
666 doi:10.1098/rspb.2011.0733.
667 Tanaka, K., M. Holcomb, A. Takahashi, H. Kurihara, R. Asami, R. Shinjo, K. Sowa, K.
668 Rankenburg, T. Watanabe, and M. McCulloch (2015), Response of *Acropora*
669 *digitifera* to ocean acidification: constraints from $\delta^{11}B$, Sr, Mg, and Ba compositions
670 of aragonitic skeletons cultured under variable seawater pH, *Coral Reefs*, *34*(4),
671 1139–1149, doi:10.1007/s00338-015-1319-6.
672 Tierney, J. E., N. J. Abram, K. J. Anchukaitis, M. N. Evans, C. Giry, K. H. Kilbourne, C.
673 P. Saenger, H. C. Wu, and J. Zinke (2015), Tropical sea surface temperatures for the
674 past four centuries reconstructed from coral archives, *Paleoceanography*, *30*, 226–
675 252, doi:10.1002/2014PA002717.
676 Toth, L. T., R. B. Aronson, K. M. Cobb, H. Cheng, R. L. Edwards, P. R. Grothe, and H.

677 R. Sayani (2015), Climatic and biotic thresholds of coral-reef shutdown, *Nat. Clim.*
678 *Chang.*, *5*, 369–374, doi:10.1038/nclimate2541.
679 Venn, A., E. Tambutte, M. Holcomb, D. Allemand, and S. Tambutte (2011), Live tissue
680 imaging shows reef corals elevate pH under their calcifying tissue relative to
681 seawater, *PLoS One*, *6*(5), e20013, doi:10.1371/journal.pone.0020013.
682 de Villiers, S., G. T. Shen, and B. K. Nelson (1994), The Sr/Ca-temperature relationship
683 in coralline aragonite: Influence of variability in and skeletal growth parameters,
684 *Geochim. Cosmochim. Acta*, *58*(1), 197–208, doi:10.1016/0016-7037(94)90457-X.
685 Weber, J. N., and P. M. J. Woodhead (1972), Temperature dependence of oxygen-18
686 concentration in reef coral carbonates, *J. Geophys. Res.*, *77*(3), 463–473,
687 doi:10.1029/JC077i003p00463.
688 Wittenberg, A. T. (2009), Are historical records sufficient to constrain ENSO
689 simulations?, *Geophys. Res. Lett.*, *36*(12), doi:10.1029/2009GL038710.
690 Wu, H. C., M. Moreau, B. K. Linsley, D. P. Schrag, and T. Corrège (2014), Investigation
691 of sea surface temperature changes from replicated coral Sr/Ca variations in the
692 eastern equatorial Pacific (Clipperton Atoll) since 1874, *Palaeogeogr.*
693 *Palaeoclimatol. Palaeoecol.*, *412*, 208–222, doi:10.1016/j.palaeo.2014.07.039.
694 Yoshinaga, J., A. Nakama, M. Morita, and J. S. Edmonds (2000), Fish otolith reference
695 material for quality assurance of chemical analyses, *Mar. Chem.*, *69*(1), 91–97,
696 doi:10.1016/S0304-4203(99)00098-5.
697 Zeebe, R. E., and D. A. Wolf-Gladrow (2001), *CO2 in seawater: equilibrium, kinetics,*
698 *isotopes*, Elsevier Science Limited.
699

700

Table 1. Summary of coral temperature, Sr/Ca and U/Ca correlations, Sr-U, and Sr/Ca

Coral	Location	Depth (m)	Mean temperature (°C)	r^2	m	Sr-U	Mean Sr/Ca (mmol mol^{-1})
Jarvis West W490	0.3696°S 160.0083°W	7	25.67 (2007-2012)	0.81	1.3 (0.4)	9.19 (0.03)	9.15
Jarvis West W497	0.3689°S 160.0081°W	16	25.67 (2007-2012)	0.64	1.9 (0.2)	9.16 (0.02)	9.25
Jarvis East 16	0.3739°S 159.9834°W	5	26.79 (2007-2012)	0.86	1.4 (0.1)	9.17 (0.02)	9.29
Jarvis East E500	0.3715°S 159.9823°W	5	26.79 (2007-2012)	0.49	2.2 (0.5)	9.12 (0.02)	9.12
Palmyra 2	5.8664°N 162.1095°W	13	28.13 (2006-2010)	0.07	5 (5)	8.98 (0.07)	9.02
Palmyra 3	5.8664°N 162.1095°W	13	28.29 (1998-2010)	0.44	2 (0.4)	8.99 (0.03)	8.89
Red Sea 1	22.0314°N 38.8778°E	1	28.41 (1998-2009)	0.23	2.3 (0.8)	9.00 (0.02)	9.02
Red Sea 44	22.0314°N 38.8778°E	5	28.41 (2005-2009)	0.46	1.8 (0.8)	8.92 (0.03)	8.97
Palau 23 (Airai)	7.3321°N 134.5602°E	4	29.18 (1997-1999)	0.36	2.0 (0.5)	8.94 (0.02)	8.89
Palau 221 (Uchelbeluu)*	7.267°N 134.521°E	5	29.26 (2008-2009)	0.79	2.5 (0.5)	8.92 (0.05)	8.66
Palau 229 (Uchelbeluu)*	7.267°N 134.521°E	5	29.26 (2008-2009)	0.79	2.5 (0.5)	8.92 (0.05)	8.82
Palau 180 (Nikko Bay)	7.3248°N 134.4684°E	6	30.04 (1997-1999)	0.29	2.0 (0.5)	8.83 (0.04)	8.94
Palau 168 (Nikko Bay)*	7.3248°N 134.4684°E	3	30.12 (2008-2009)	0.30	1.8 (0.9)	8.78 (0.07)	8.66
Palau 169 (Nikko Bay)*	7.3248°N 134.4684°E	6	30.12 (2008-2009)	0.30	1.8 (0.9)	8.78 (0.07)	8.72
Literature data:							
[*Cardinal et al.,* 2001]							
Bermuda N Rocks	32.5°N 64.67°W	24	23.0 (1971-1984)	0.67	2.1 (0.4)		
Bermuda NE Breakers	32.5°N 64.67°W	11	22.9 (1981-1984)	0.49	1.9 (0.6)		
[*Quinn and Sampson* 2002]							
New Caledonia	22.48°S 116.47°E	3	24.7 (1968-1990)	0.52	1.6 (0.2)		
[*Felis et al.,* 2009]							
Japan	27.106°N 142.194°E	6	24.3 (1982-1994)	0.88	1.6 (0.1)		

Notes: Coefficient of determination (r^2) and slope (m) of Sr/Ca vs U/Ca relationship determined by reduced major axis regression. Parentheses indicate ± 2σ. Sr/Ca and U/Ca are significantly correlated in all of these corals..

* Palau 168 and 169 (Nikko Bay), and Palau 221 and 229 (Uchelbeluu) were grouped together to calculate Sr-U.

701

702

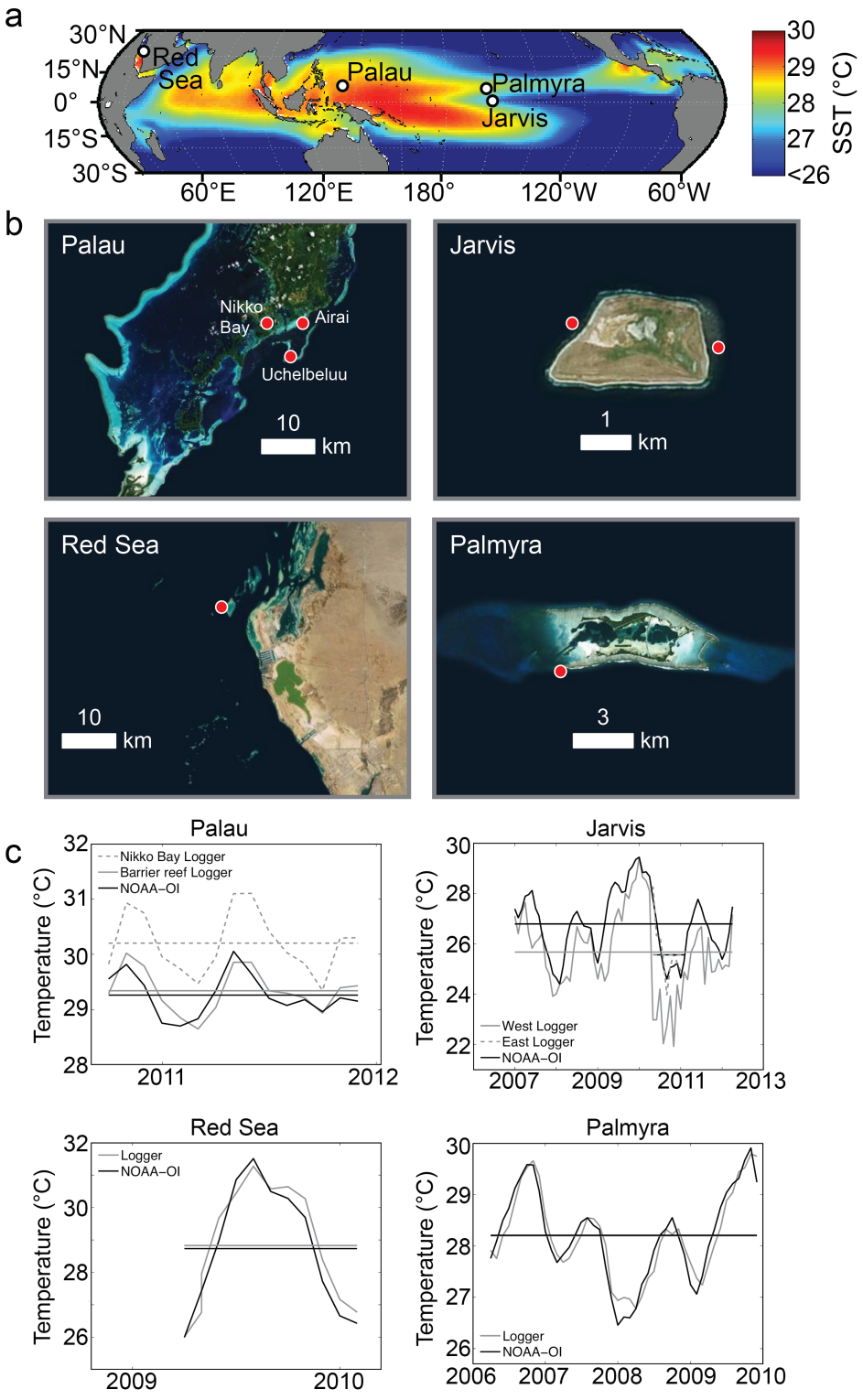

703

704 Figure 1. Coral sampling locations and sea surface temperatures. (a) Map of

705 climatological mean (1971-2000) sea surface temperature (SST) from the NOAA-OI

706 dataset, with coral reef sampling locations indicated by white dots. (b) Satellite images of
707 each reef, with locations of coral sampling indicated by red dots. (c) Comparisons
708 between NOAA-OI and *in situ* logger temperatures for each coral sampling location.
709 Horizontal bars indicate mean temperature for each location.
710

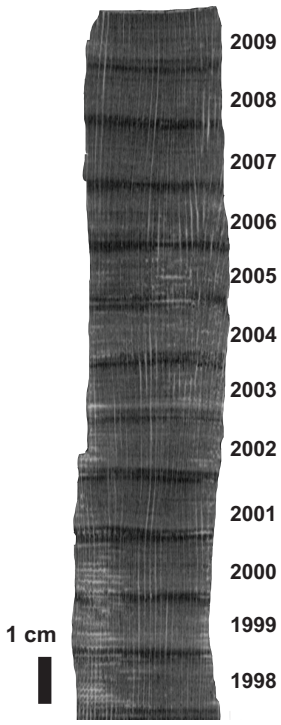

711

712 Figure 2. Computerized tomography (CT) scan of Palmyra 3 coral. Light (dark) shading
713 indicates relatively high (low) density skeleton. The timescale is derived from annual
714 density banding, visible as approximately horizontal alternating low- and high-density
715 bands.
716

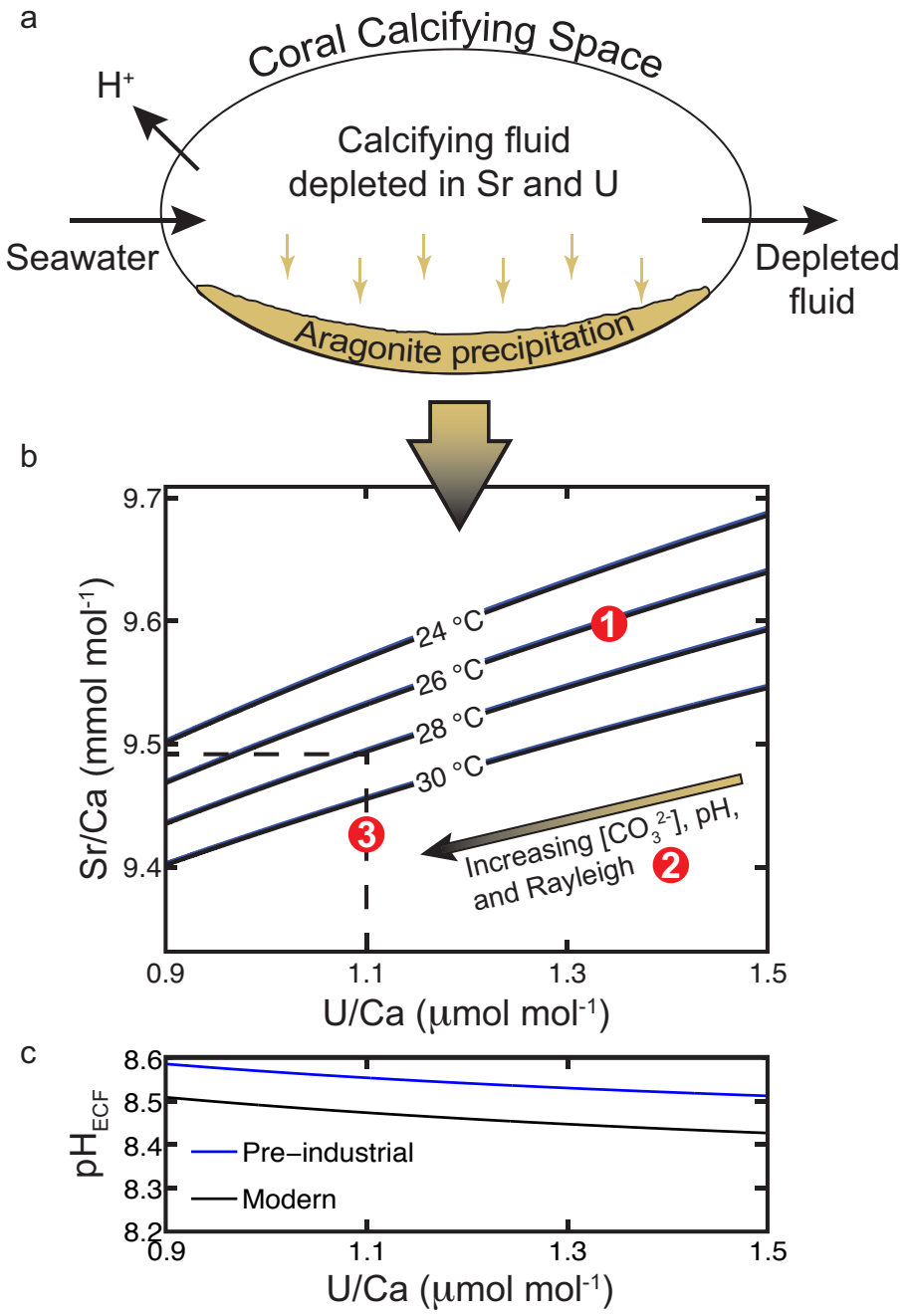

717

718 Figure 3. Coral biomineralization model. (a) Schematic diagram of semi-isolated coral

719 calcifying space where the fluid in the space is supplied by seawater and elemental

720 concentrations of the fluid are depleted relative to seawater as aragonite precipitates.

721 Removal of protons (H^+) from the fluid represents alkalinity pumping. (b) The model of

722 *DeCarlo et al.,* [2015a] is evaluated between 24 °C and 30 °C (solid black lines, each

representing the relationship between Sr/Ca and U/Ca at a specific temperature) and plotted for U/Ca ratios consistent with *Porites* coral skeleton (0.9 to 1.5 μmol mol^{-1}). Red circles indicate the three predictions of the model that we test with coral data: (1) skeleton Sr/Ca and U/Ca ratios are positively correlated, (2) increasing Rayleigh fractionation, combined with increasing ECF pH and $[CO_3^{2-}]$, decreases both skeleton Sr/Ca and U/Ca ratios, and (3) at a specific skeleton U/Ca ratio (dashed line), Sr/Ca depends only upon temperature. (c) Predicted calcifying fluid pH and coral skeleton U/Ca ratio at salinity 35 and temperature of 25 °C, and assuming ambient seawater total alkalinity of 2300 μeq kg^{-1}, and $[CO_3^{2-}]$ of pre-industrial (blue) and today (black) based on *Feely et al.,* [2009]. While the absolute pH_{ECF} at a particular U/Ca ratio is sensitive to ambient seawater $[CO_3^{2-}]$, the model consistently predicts increasing pH_{ECF} with decreasing Sr/Ca and U/Ca ratios. Critically though, seawater $[CO_3^{2-}]$ has little influence on Sr-U temperature sensitivity, and the industrial $[CO_3^{2-}]$ change would shift the isolines in panel (b) by the equivalent of only ~0.03 °C (note that the blue and black lines representing the two $[CO_3^{2-}]$ scenarios are partially overlapping in panel b).

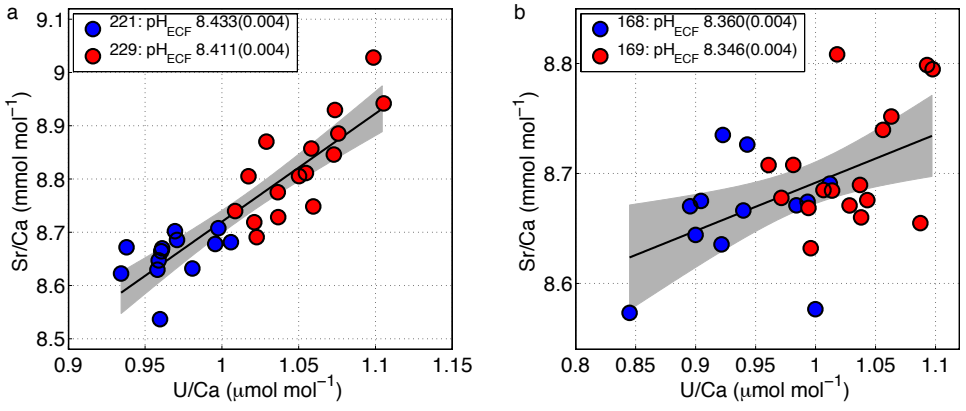

740 Figure 4. Vital effects in two pairs of corals, each pair collected from a single reef in
741 Palau and sampled over the same time period (2008-2009). Property-property plots of
742 Sr/Ca and U/Ca ratios from corals collected in (a) Uchelbeluu (corals "221" and "229")
743 and (b) Nikko Bay (corals "168" and "169"). Sr/Ca and U/Ca ratios of corals collected
744 from a single reef are positively correlated. Within each pair of corals from a single reef,
745 lower Sr/Ca and U/Ca ratios are correlated with elevated pH_{ECF}. The pH_{ECF} is reported as
746 the mean with the number in parentheses indicating the standard error of the mean. Solid
747 black lines with gray bounds indicate least squares regression and 95% confidence
748 interval between Sr/Ca and U/Ca ratios. Note that the scales are different between the
749 panels in order to aid interpretation of the plots. Time series plots of these data are
750 displayed in supplementary Figure S1.
751

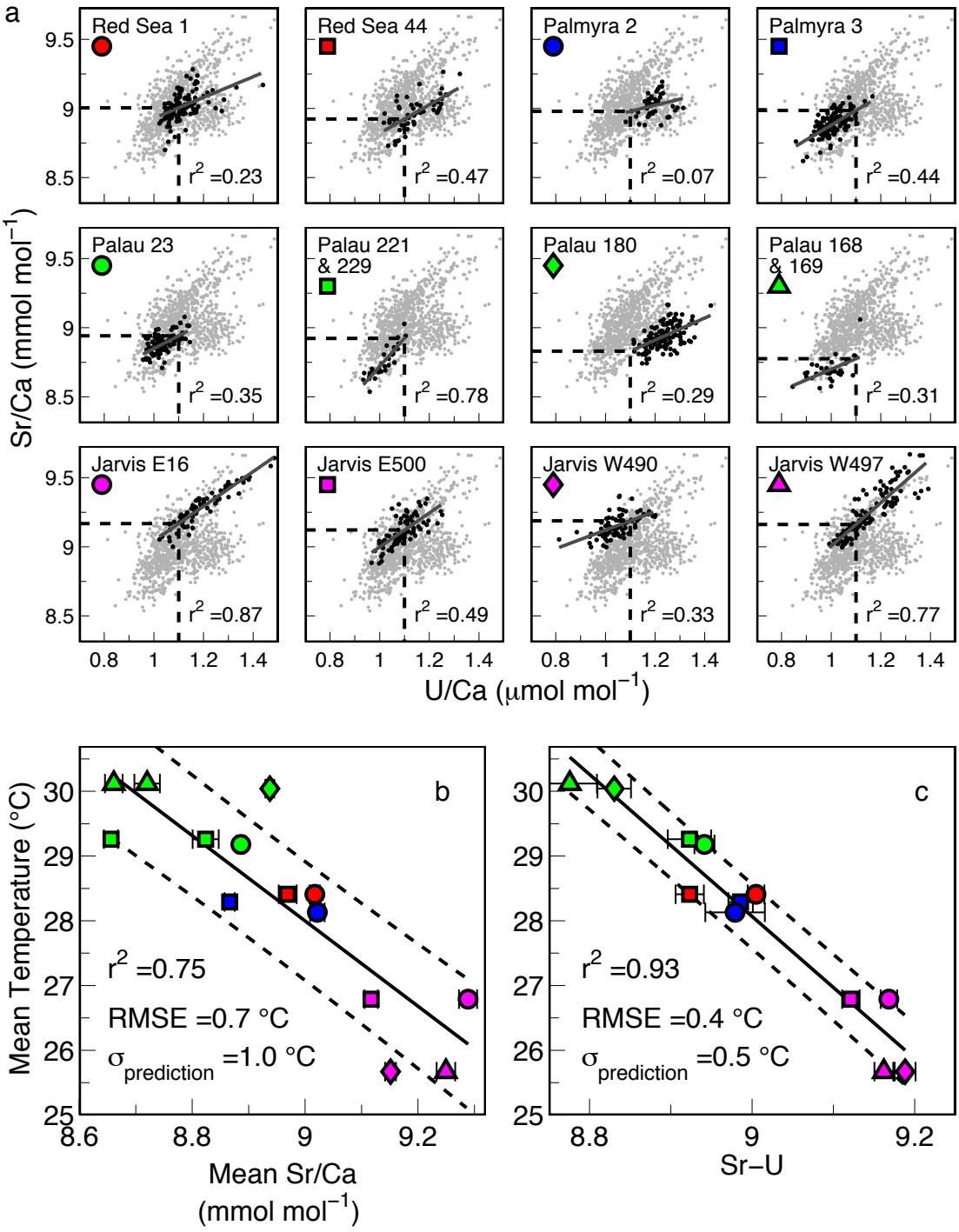

752

753 Figure 5. Calibration of the Sr-U thermometer. (a) Sr/Ca and U/Ca relationship of 14

754 *Porites* colonies from the Pacific Ocean and Red Sea. Each panel shows the data for a

755 given coral in black and all other corals in light gray. The trend lines for each coral were

fit by ordinary least squares regression between Sr/Ca and U/Ca (solid dark gray lines). Sr-U is the estimated Sr/Ca at U/Ca of 1.1 μmol mol^{-1} (dashed lines). The colored symbol below the name of each coral indicates its position on the calibration plots in panels (b) and (c). Palau 221 and 229 (Uchelbeluu), and Palau 168 and 169 (Nikko Bay) data are each grouped from two separate corals collected on the same reefs because one coral from each location did not include U/Ca ratios as high as 1.1 μmol mol^{-1} needed to define Sr-U. (b) Mean Sr/Ca and (c) Sr-U for each coral regressed with mean annual temperature. Dashed lines in (b) and (c) show 1 σ of prediction. Horizontal error bars in (b) show standard error of mean Sr/Ca, and in (c) show the 1 σ uncertainty of the Sr/Ca and U/Ca regression at U/Ca of 1.1 μmol mol^{-1}.